The Impact of Dam Construction on Downstream Vegetation Area in Dry Areas Using Satellite Remote Sensing

Raid Almalki , Mehdi Khaki * , Patricia Saco , Jose Rodriguez

Posted Date: 8 August 2023

doi: 10.20944/preprints202308.0566.v1

Keywords: Vegetation areas; Satellite remote sensing; Downstream vegetation; Climate variability; Arid regions

Article

The Impact of Dam Construction on Downstream Vegetation Area in Dry Areas Using Satellite Remote Sensing

Raid Almalki [1,2], Mehdi Khaki [2,*], Patricia M. Saco [2] and Jose F. Rodriguez [2]

[1] School of Environmental and Life Science, University of Newcastle, Callaghan, NSW 2308, Australia
[2] Department of Geography, Umm Al-Qura University, Makkah 21955, Saudi Arabia
[3] School of Engineering, University of Newcastle, Callaghan, NSW 2308, Australia
* Correspondence: mehdi.khaki@newcastle.edu.au

Abstract: The assessment of ecosystem quality and the maintenance of optimal ecosystem function requires understanding vegetation area dynamics and its relationship with climate variables. This study aims to detect vegetation area changes over a downstream dam and to understand the influence of the dam as well as climatic variables on the region's vegetation areas. The case study is located in an arid area with an average rainfall amount of 50 to 100 mm/year. An analysis of seasonal changes in vegetation areas was conducted using the Normalized Difference Vegetation Index (NDVI), and supervised image classification was used to evaluate changes in vegetation areas using Landsat imagery. Pearson correlation and multivariate linear regression were used to assess the response of local vegetation areas to both hydrologic changes due to dam construction and climate variability. The NDVI analysis reveals a considerable vegetation decline after the dam construction in the dry season. This is primarily associated with the impoundment of the seasonal water by the dam and the increase in cropland areas due to dam irrigation. A significantly stronger correlation between vegetation changes and precipitation and temperature variations is observed before the dam construction. Furthermore, multivariant linear regression was used to evaluate the variations of equivalent water thickness (EWT), climate data, and NDVI before and after the dam construction. The results suggest that 85 percent of the variability in the mean NDVI was driven by climate variables and EWT before the dam construction. On the other hand, it was found that only 42 percent of the variations in NDVI were driven by climate variables and EWT after the dam construction for both dry and wet seasons.

Keywords: vegetation areas; satellite remote sensing; downstream vegetation; climate variability; arid regions

1. Introduction

Vegetation is one of the most fundamental parts of the earth's ecosystem (Jiang et al., 2017). Quantitative measurements of vegetation areas on well-defined spatiotemporal scales are important for ecological and climatological studies (Soepboer et al., 2010). The Normalized Difference Vegetation Index (NDVI) is an indicator of vegetation's ability to absorb photosynthetically active radiation and is the most widely used vegetation index to analyze vegetation dynamics (Wang et al., 2003). The index measures the reflectance of vegetation in the red and near-infrared bands (Bhandari et al., 2012; Nageswara Rao et al., 2005). It is applied primarily in both global and regional studies, to understand and quantify the impact of climate variables on vegetation productivity, phenology, and how vegetation responds to other factors and stressors (Gandhi et al., 2015). Studying vegetation areas changes over arid and semi-arid regions, however, is very challenging. The vegetation areas in these regions is widely recognized as a complex system due to the water-stress, and its low density and sparse distribution (Li et al., 2005). Plant growth is limited in arid regions by a lack of

precipitation and humidity combined with relatively high temperatures and evapotranspiration, which is sometimes highly dependent on global and local climate (Xu et al., 2016).

Many studies have shown the complexity of studying NDVI changes and their relationship with climate variabilities over semi-arid and arid regions (Foody, 2003). Wang et al. (2003) investigated the correlation between NDVI and temperature and precipitation in the central United States Great Plain. A high correlation was found between NDVI values during the growing season (March–October) and precipitation. Early and late in the growing season, NDVI correlated positively with temperature; however, in the middle, it correlated negatively (Wang et al., 2003). A study by Xie et al. (2016) found that temperature positively correlates with vegetation in most periods in semi-arid areas. In the Xinjiang desert of northwest China, vegetation has primarily shown a greening curve in recent decades, and the primary variable driving this process, as identified, is precipitation (Shi et al., 2007; Zhou et al., 2014). Kumari et al. (2020) investigated the effect of aspect-driven soil moisture differences on semiarid ecosystems using NDVI metrics. This study identified the existence of a seasonal reversal in higher vegetation greenness between polar-facing slopes and equatorial-facing slopes. Tong et al. (2018) mentioned that NDVI correlated positively with precipitation and temperature in the Inner Mongolian desert, where precipitation has a more substantial effect on vegetation variation than temperature.

Moreover, the impact of large dams can pose further difficulties in studying vegetation variation in dry areas by disrupting the water runoff downstream. Various studies indicate different connections between local climate change and dam construction through the analysis of precipitation and temperature changes (see, e.g., Khaki & Hoteit 2021). According to Degu et al. (2011), large dams in Mediterranean climates have the most significant effect on the climate closer to reservoir areas and negligible influence in a humid subtropical climate. Based on the study results, Zhao et al. (2021) concluded that Miyun Reservoir (catchment area around 15,788 km^2) significantly impacted both temperature and precipitation during the summer half. A study by Chen (2015) found that precipitation had not changed significantly, but the temperature had risen since the Three Gorges Reservoir (catchment area around 1 million km^2) was impounded. However, according to Miller et al. (2005), and based on multiple experiments to simulate the effects of the Three Gorges Reservoir on the local climate within 10 km, no effects on precipitation were found. But a different study by Wu et al. (2006), found that there is an effect on precipitation at the regional scale of 100 km rather than at the local scale.

The main objective of this study is to analyze the impact of the Hali dam construction on downstream vegetation areas using satellite remote sensing. In addition, it investigates the potential impact of the local climate on downstream vegetation areas over the Wadi Hali basin, located in Saudi Arabia. Due to its highly arid conditions, the Hali basin's climate is characterized by a harsh combination of extreme heat, high evaporation, and limited surface water. Furthermore, it is characterized by a long dry season marked by severe drought and a short wet season with irregular rainfall (Hasanean & Almazroui, 2015). Geographic information systems (GIS) and remote sensing were used to study the vegetation areas changes and the corresponding impact of local climate variabilities. GIS and remote sensing provide essential data and tools for spatiotemporal detection modeling at a local and global scale for the past, current, and future. Several changes in vegetation can be detected and monitored through remote sensing, including changes in aboveground production, structure, and cover (Almalki et al., 2022). Vegetation areas change detection is critical for understanding the interaction and interrelationships of the ecosystem, climate, and human activities. Monitoring vegetation changes at different spatial and temporal scales using this technique is also important to detect changes in vegetation structure, function, and interaction with climate variabilities (Ahmed, 2018; Belal et al., 2014; Murray & Khaki 2021).

Previous studies have investigated NDVI and climate variables using various variables such as sunshine, wind velocity, and directions, allowing them to measure NDVI's determinants with good precision (Hu et al., 2011). Nevertheless, temperature and precipitation have been found to be the two most used (Hu et al., 2011). Srivastava et al. (1997) investigated semi-arid dryland areas in six districts in India, and they found that NDVI has a much stronger relationship with the amount of

Preprints (www.preprints.org) | NOT PEER-REVIEWED | Posted: 8 August 2023 doi:10.20944/preprints202308.0566.v1

water consumed by vegetation than precipitation. Moreover, a study by Ji and Peters (2004), which used six climate variables to analyze the grasslands of the United State Great Plains, water condition was the most important factor in determining vegetation growth. This study uses Landsat imagery time series to detect vegetation areas changes downstream of the Hali dam in the Wadi Hali basin and further explores the influence of the climate variables and equivalent water thickness (EWT) on the downstream vegetation areas. Climate variables used in this study include two-meter surface temperature, total precipitation, total evaporation, and specific humidity.

2. Case study

The Wadi Hali basin is located within the Asir mountains and near the Red Sea coast (Alarifi et al., 2022), in the southwestern region of Saudi Arabia. It is one of the largest wadis in Saudi Arabia, located in the Southern Tihama Plain, with an average slope of 17.5 m/km and a total length of 160 km. The study area is in a hot desert climate based on (Hasanean & Almazroui, 2015), and this type of climate contains two types of seasons: long summers and short winters. Precipitation from the adjoining hills is collected within the watersheds and channeled toward the Red Sea (Alarifi et al., 2022). The Hali basin has an average rainfall amount of 50 to 100 mm/year, and the headwaters of the Hali basin have an average rainfall amount of 300 to 600 mm/year (Hasanean & Almazroui, 2015). The Hali Dam is in the Wadi Hali basin on the Red Sea coast on the southwestern side of the Kingdom of Saudi Arabia at Longitude 41°30′00″ E and Latitude 18°44′00″ N. The Red Sea coast of the Arabian Peninsula contains different ravines along the coast and has a limited amount of vegetation except for a few sparse species of Prosopis Juliflora, halophytes and mangroves (Avicennia marina). The Hali Dam is a gravity dam constructed in 2009 and has a catchment area of 5,222 km^2 (Alarifi et al., 2022). According to the Ministry of Environment, Water, and Agriculture in Saudi Arabia, several dam applications are flood control, irrigation, domestic water supply, and groundwater recharge. The dam has a total storage of 249,860,000 m^3 (Alarifi et al., 2022). Its headwaters are located at an elevation of about 2,000 m above mean sea level, extending west to the red sea.

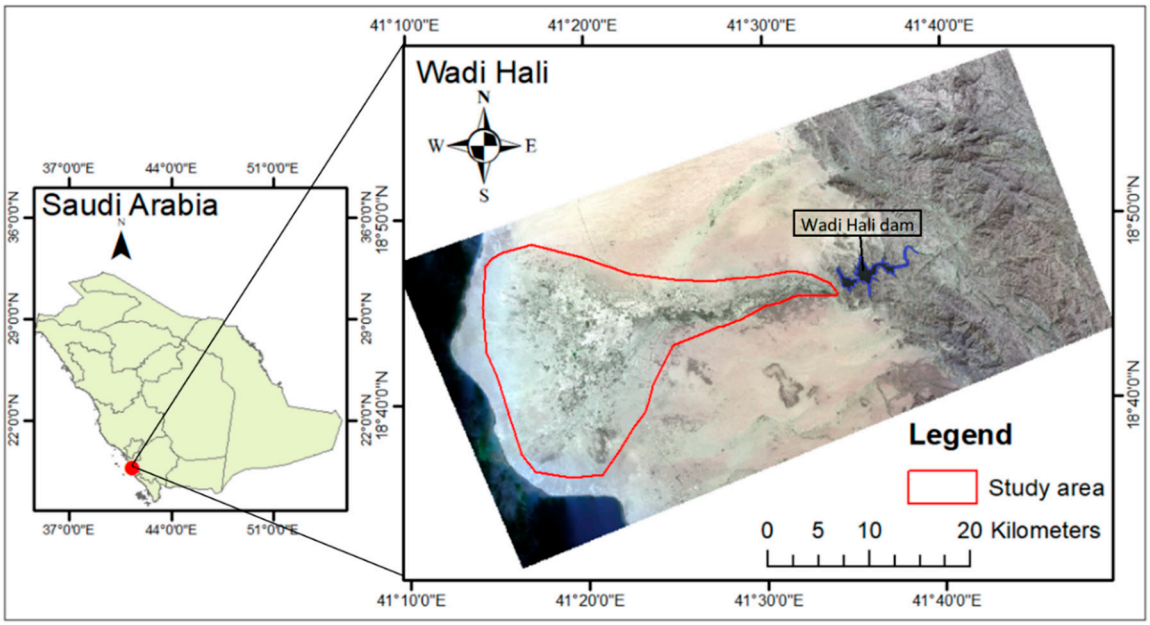

Figure 1. The geographical location of the study area.

 doi:10.20944/preprints202308.0566.v1

3. Database

3.1. Satellite Data Source and Pre-Processing

The Landsat satellite images, including Thematic Mapper, Enhanced Thematic Mapper Plus, and Operational Land Imager, were obtained from the United States Geological Survey (USGS). All images were acquired in levels and collections 1 and were radiometrically and atmospherically corrected. In this study, satellite images were selected based on three criteria: (1) cloud coverage of the satellite images must be less than 10 percent, (2) the availability of images satellite series should be available over a long period to have the ability to compare downstream changes before and after the dam construction, and (3) the data should be available over wet and dry seasons. Satellite images were selected mainly for January and February for the wet season from 2000 to 2020. During the dry season from 2000 to 2020, satellite images were selected mainly for August and September. During these months, the most data are available in terms of availability, and these months were chosen because they represent the peak of each season.

3.2. Climate Variables Selection and Data

Climatological data variables such as temperature, precipitation, humidity, evaporation, and wind speed are important parameters that describe a specific region's climate. The study area is located in an arid area, where the climate tends to be characterized by low precipitation and high temperatures, and both profoundly affect vegetation growth, making ecosystems more vulnerable to climate change (Han et al., 2021). In this study, temperature, precipitation, specific humidity, and evaporation were considered to investigate the impact of climate variables on vegetation areas activities. We considered climate data for the dry season from May to September and the wet season from October to February to investigate vegetation areas response to climate variability. Climate data were acquired from the European Centre for Medium-Range Weather Forecasts Integrated Forecasting System, the fifth-generation reanalysis ERA-5, and the Global Land Data Assimilation System (GLDAS), which have widely been used in previous studies (Khaki et al., 2015; Zhong et al., 2019). This study used 21 years of climatic data, including two-meter surface temperature, evaporation, and total precipitation from ERA-5 and specific humidity from GLDAS for the period of 2000 to 2020 with 0.1° × 0.1° spatial resolution and monthly averaged time frequency.

3.3. Equivalent Water Thickness (EWT)

Gravity field variations due to Earth's mass changes were obtained from The Gravity Recovery and Climate Experiment (GRACE) mission (Xie et al., 2019). Gravitational variations measured by GRACE are primarily due to water distribution on and beneath the earth's surface over the terrestrial area (Borsa et al., 2014). Therefore, it can estimate the vertical changes in terrestrial water storage, including surface water, soil moisture, groundwater, canopy storage, and snow water equivalent (Xie et al., 2019). In this study, we used the monthly EWT product of JPL MASCON GRACE product Level-3 data (source: grace.jpl.nasa.gov) for the study area for the (available) period from April 2002 to December 2020.

4. Methods

Figure 2 summarizes the research method starting from collecting the data, including Landsat imageries and climate data from ERA-5 and GLDAS models. Online acquisition of EWT data was conducted. All the imagery data was pre-processed, such as radiometric, geometric, and atmospheric corrections, which is a crucial step in preparing the data before analysis. The NDVI calculation and supervised classification using Maximum Likelihood Classification (MLC) were applied to satellite imagery before and after dam construction. A high spatial resolution Satellite pour l'Observation de la Terre (correlation) image was used to evaluate the accuracy of the supervised classification. Change detection maps were produced before and after dam construction (2000–2009 and 2009–2020, respectively). Afterwards, Pearson correlation analysis and linear regression analysis were used to

Preprints (www.preprints.org) | NOT PEER-REVIEWED | Posted: 8 August 2023 doi:10.20944/preprints202308.0566.v1

explore the relationship between the vegetation data acquired from satellite imagery and both climate and EWT data. In the following sections, all the steps taken to obtain the results presented in this study are explained in more details.

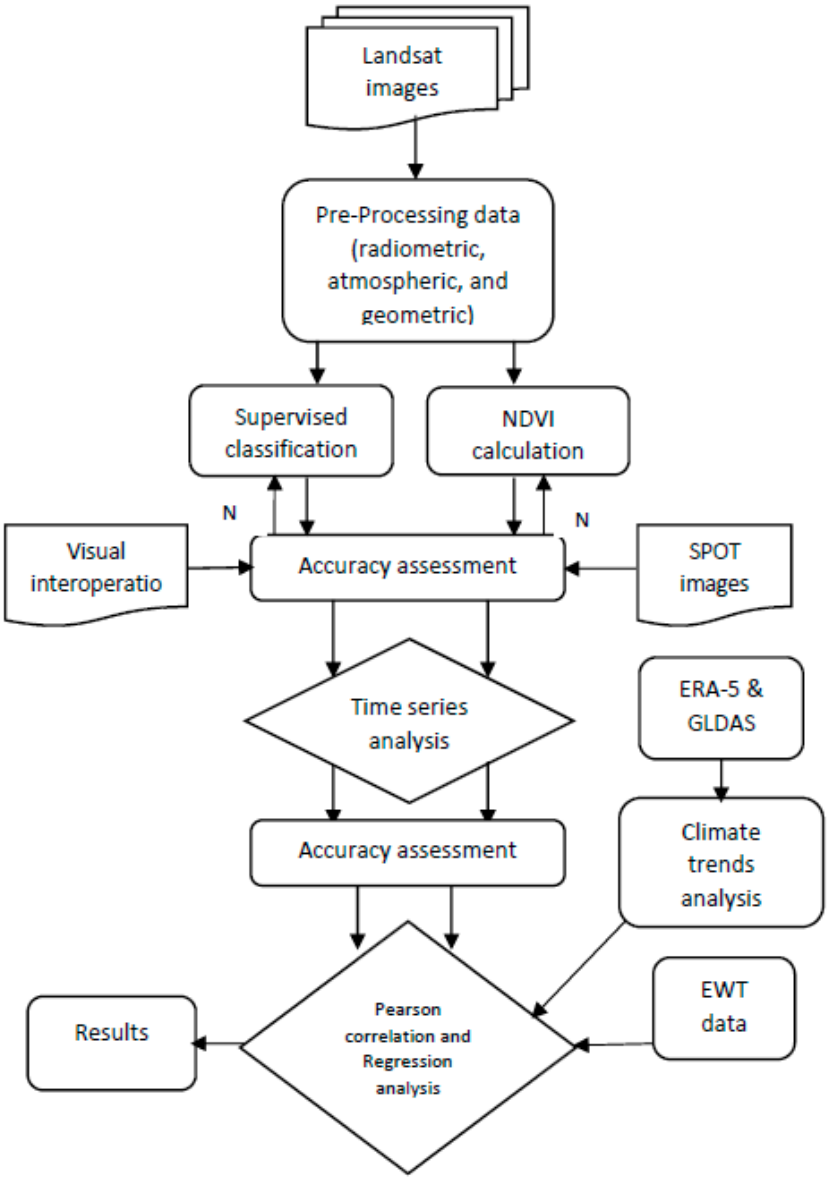

Figure 2. Flowchart of the applied methodology to analyse the vegetation changes in the Wadi Hali basin before and after the Hali dam construction.

4.1. Image Classification

4.1.1. Maximum Likelihood Classification (MLC)

MLC is one of the most commonly used parametric classifiers (Otukei & Blaschke, 2010) to investigate different vegetation types (e.g., natural vegetation and croplands) changes. In this method, pixels are classified based on their probability of belonging to a particular class. The covariance matrix is used to account for the variability of classes. For the MLC algorithm to perform correctly, it needs enough training sample plots with representative spectral signatures for each class. More details can be found in different textbooks, such as (Richards & Richards, 1999). Landsat images were classified using MLC, into natural vegetation, croplands, and bare areas.

4.1.2. Accuracy Assessment

Performing an accuracy assessment is an essential step for the evaluation of the classification results. As vegetation areas changes, it is crucial to know the accuracy of the result before using it (Mohajane et al., 2018). A confusion matrix, which is an array of numbers arranged in rows and columns that indicates how many sample units (pixels) are assigned to each category compared to what is actually in the ground, was used here. Moreover, is often used to derive descriptive and analytical statistics to determine classification accuracy. The high spatial resolution SPOT images acquired from King Abdulaziz City for Science and Technology of (1.5 to 10 m) for 2004, 2006, 2012, 2016, and 2021 were used to produce a stratified random sample for each vegetation class. Each image was used for accuracy assessment evaluation for the corresponding years, assuming that no significant changes accrued within the seasons. Many samples were taken to attain high classification and accuracy results. Overall, 116 samples were considered for each year in each season to produce accurate assessment results.

4.2. NDVI Calculation

NDVI is an index that is widely used to describe vegetation variations. NDVI is used to enhance the presence or absence of vegetation by generating the normalized band ratio. NDVI values range from +1 to −1, where positive values represent green cover while negative values indicate non-vegetative surfaces (Almalki et al., 2022). The higher the positive values, the more vegetation there is. The negative NDVI describes water bodies, built-up areas, while bare areas range from 0 to 0.03, and the values for healthy vegetative typically are between 0.4 and 0.76 for cropland and natural vegetation (Zaidi et al., 2017).The NDVI index is calculated using the following equation:

$$\text{NDVI} = (\text{NIR}-\text{RED})/(\text{NIR}+\text{RED}) \quad (1)$$

In the case of Landsat-5 and 7, near-infrared (NIR) indicates band four, and Red (RED) indicates band 3. Regarding Landsat-8, near-infrared (NIR) indicates band five, and Red (RED) indicates band 4. NDVI was calculated as seasonal (wet and dry) and annual by combining wet and dry seasons for each year from 2000 to 2020. NDVI was calculated 9 years and 12 years before after dam construction, respectively. After the NDVI values are calculated for each season in every year, the mean NDVI is calculated before and after dam construction.

The value of $NDVI_d$, obtained as the difference between the mean NDVI before ($NDVI_{mean\ before}$) and after ($NDVI_{mean\ after}$) dam construction is calculated for each season using Equation 2. The results are presented as two maps illustrating each season's gain and loss of vegetated cover areas.

$$NDVI_d = NDVI_{mean\ after} - NDVI_{mean\ before} \quad (2)$$

4.3. Pearson's Correlation Coefficient

The Pearson's correlation coefficient evaluates the strength of the linear relationship between two variables by using the covariance matrix of the data and computed using Equation (3).

$$r = \frac{\sum(xi-\overline{x})^2 \sum(yi-\overline{y})^2}{\sqrt{\sum(xi-\overline{x})^2 \sum(yi-\overline{y})^2}} \quad (3)$$

Where r is the correlation coefficient between x and y, which represent the values of the vegetation variable (natural vegetation, cropland, and mean NDVI) and the climate variable (temperature, precipitation, specific humidity, or evaporation), respectively. i represents the years and $\overline{x}$ and $\overline{y}$ are the average monthly values of the vegetation and climate variables, respectively.

This study used Pearson's correlation coefficient to analyze the relationship between vegetation types (i.e., natural vegetation, croplands, and mean NDVI), climate variables (i.e., two-meter surface temperature, precipitation, specific humidity, and evaporation), and EWT. This is to identify the major climate variables that have impacted the vegetation areas of the study area from 2000 to 2020. The Pearson's correlation coefficient was applied to the time series for each season before and after

 doi:10.20944/preprints202308.0566.v1

the dam construction as well as the p-value to test whether the observed correlation between two variables is statistically significant.

4.4. Multivariate Regression Analysis

The final step of this study was applying the multivariate regression analysis, which can determine the relationships between two or more variables leading cause-effect understanding (Tranmer & Elliot, 2008). Climate variables and water in the soil are one of the important driving forces for vegetation growth. Therefore, multivariate regression analysis was applied to NDVI using climate variables and to evaluate if the variations of EWT and climate variables data could explain the NDVI variability before and after the dam construction. The first multivariate regression analysis was done before the dam construction from 2002 to 2009 and the second one was applied after the dam construction from 2010 to 2020. The results are presented to assess the ability of EWT and climate variables data to predict the NDVI variations over the two periods. The multivariate regression analysis model (Equation 4) is estimated by,

$$y = \beta_0 + \beta_1 x_1 + \beta_2 x_2 + \beta_3 x_3 + \beta_4 x_4 + \beta_5 x_5 + e \quad (4)$$

In equation (4), y represents the dependent variable (mean NDVI) and x represents the independent variables (EWT, two-meter surface temperature, precipitation, evaporation, and specific humidity). β_0 is the intercept of y, and β_x is the changes in the mean of y or represents the slope of the regression line. e represents the model's equation error.

5. Results

5.1. Annual and seasonal variation of vegetation areas:

5.1.1. Vegetation areas using supervised classification (MLC)

The vegetation areas classification maps for the years 2000 to 2020 for wet and dry seasons produced from Landsat images are displayed in Figures 3 and 4, respectively. The figures illustrate the results for five years (2000, 2005, 2010, 2015, and 2020) and for the two seasons. The supervised classification shows natural vegetation and croplands. The vegetation areas of the study area changed considerably between 2000 and 2020 for both seasons. The average area covered by natural vegetation decreased by 25.5 percent from 2000 to 2020, while croplands increased by 48.4 percent from 2000 to 2020. Moreover, comparison of results before and after the dam construction, show that the average area covered by natural vegetation declined by 28.4 percent after the dam construction. In contrast, the croplands increased by 62.7 percent after the dam construction. The increase in croplands could be due to various reasons, but irrigation plays a significant role as it was one of the important reasons for dam construction. This caused an increased in croplands and a decrease in natural vegetation areas due to the dam's impoundment of seasonal water flow after heavy rain, which used to support natural vegetation before the dam construction.

Preprints (www.preprints.org) | NOT PEER-REVIEWED | Posted: 8 August 2023 doi:10.20944/preprints202308.0566.v1

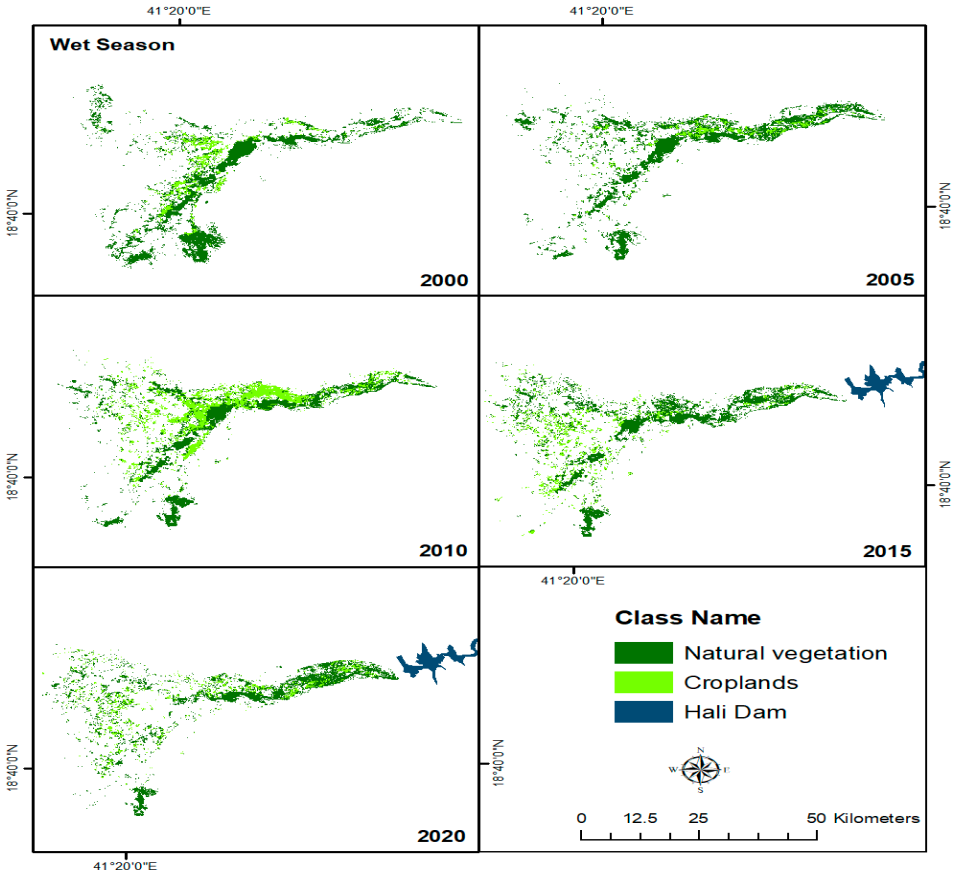

Figure 3. Supervised classification of the variation of the spatial distribution of vegetation areas for wet seasons for 2000, 2005, 2010, 2015, and 2020.

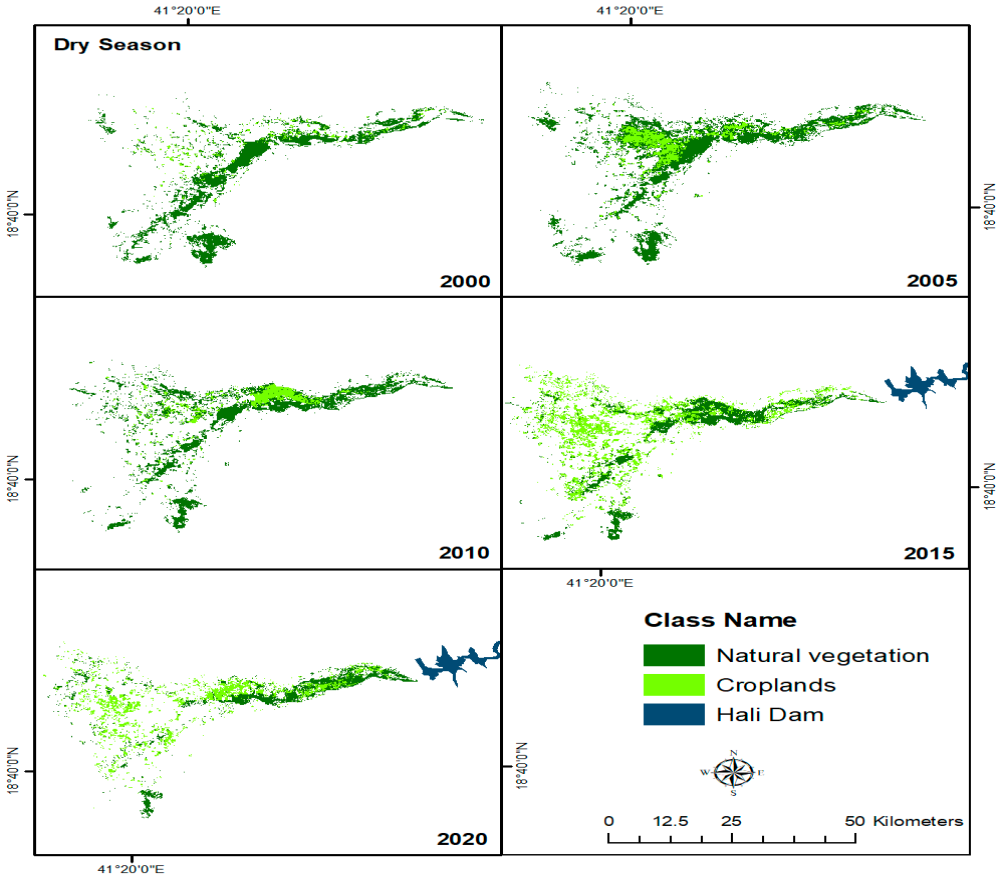

Preprints (www.preprints.org) | NOT PEER-REVIEWED | Posted: 8 August 2023 doi:10.20944/preprints202308.0566.v1

Figure 4. Supervised classification of the variation of the spatial distribution of vegetation areas for dry seasons for 2000, 2005, 2010, 2015, and 2020.

Figure 5 shows the bar chart of total natural vegetation and cropland areas in km² over study sites for the wet and dry seasons and for the period 2000 to 2020. Before the dam construction (2009), the natural vegetation and croplands slightly increased in the two seasons. After the dam construction, the trend line decreases for natural vegetation and increases for the croplands in both seasons. Prior to dam construction, there was an increase of 681 km² and 600 km² in natural vegetation areas during wet and dry seasons, respectively. Following dam construction, natural vegetation areas experienced decrease of 1116 km² and 479 km² during wet and dry seasons, respectively. On the other hand, before the dam construction, there was an increase of 222 km² and 1171 km² in cropland areas during wet and dry seasons, respectively. Following dam construction, cropland areas experienced increases of 1209 km² and 1758 km² during wet and dry seasons, respectively The main crops grown in this region are sorghum, sesame, and millet (Morgounov et al., 2022). These crops are warm season plants and their growth usually from May to October (Guarino & Al-Juwaeid, 1990). The cropland variation is significantly higher in the dry season compared to the wet season due timing of the growing season. The results suggest that the changes in the natural vegetation and croplands are associated with dam construction. The decrease in the natural vegetation after the dam construction could be due to the impoundment of the seasonal water flow by the dam construction. Moreover, the significant increase in the croplands after the dam construction could be associated with water management policies and dam applications, such as releasing water for agricultural irrigation from the dam.

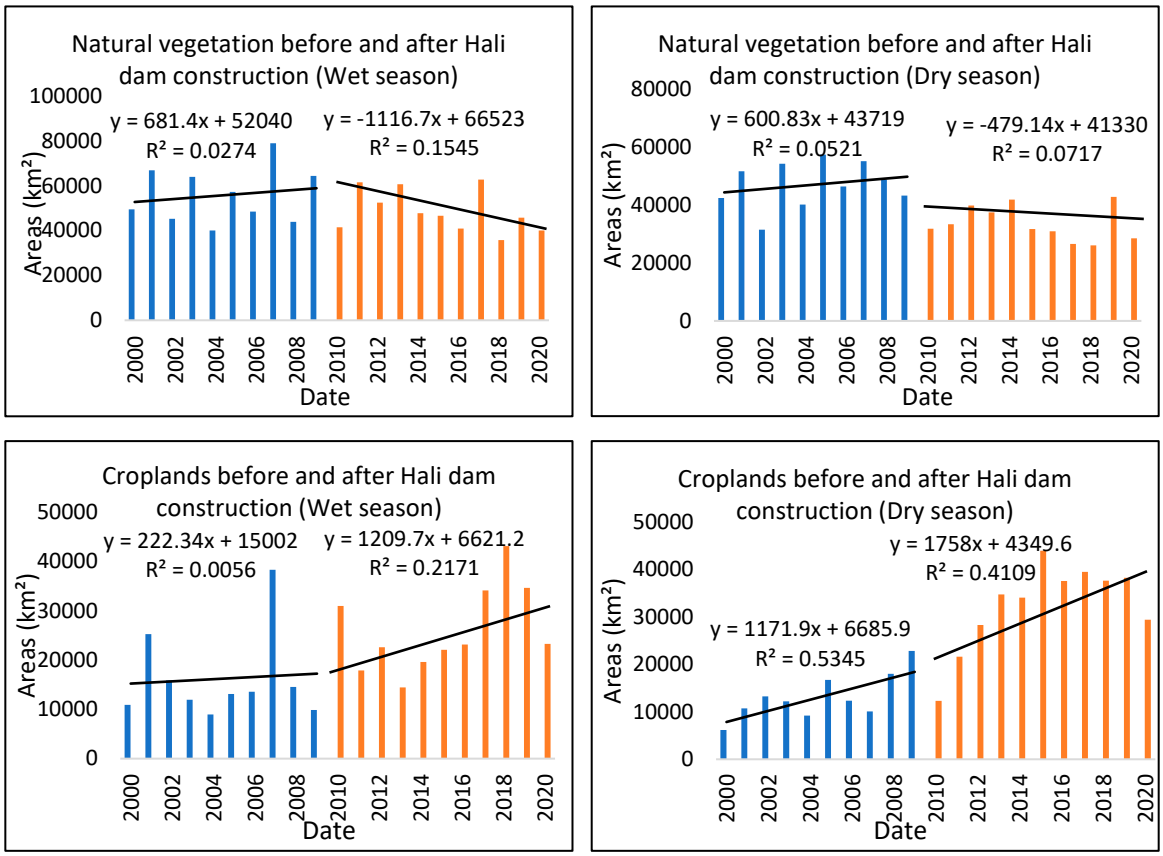

Figure 5. The total areas of natural vegetation and croplands before and after the dam construction for wet and dry season.

Preprints (www.preprints.org) | NOT PEER-REVIEWED | Posted: 8 August 2023 doi:10.20944/preprints202308.0566.v1

5.1.1. Accuracy assessment of vegetation areas using supervised classification

As a result of the accuracy assessment of the image classifications, it was determined that the overall accuracy of the supervised classification was between 71 percent and 92 percent across all seasons. The accuracy assessment results were calculated using a confusion matrix and high spatial resolution of satellite imageries (SPOT) for 2004, 2006, 2012, 2016, and 2021 between image pixels to the actual feature in the ground, as in Table 1. As mentioned by (Congalton, 1991), an accuracy assessment value greater than 70 percent is considered acceptable to represent a perfect correspondence. In comparison, an accuracy assessment of less than 70 percent could indicate confusion between vegetation areas types in the classification results. All the accuracy values in Table 1 are acceptable because they are higher than 70 percent. The average accuracy value for the wet season is 76 percent and 79 percent for the dry season. The highest accuracy was associated with the same years of the SPOT imagery that was used for accuracy assessment classification, such as 2004, 2012, and 2016. However, the lowest accuracy values were associated with the years that did not have the same years of SPOT imagery used for accuracy assessment classification.

Table 1. Supervised classification accuracy assessment results.

Year	Wet season	Dry Season	Year	Wet season	Dry Season
2000	81%	73%	2011	73%	80%
2001	73%	73%	2012	76%	92%
2002	72%	80%	2013	74%	82%
2003	75%	72%	2014	71%	80%
2004	79%	80%	2015	76%	81%
2005	78%	78%	2016	80%	82%
2006	76%	76%	2017	78%	78%
2007	78%	73%	2018	74%	80%
2008	75%	79%	2019	92%	87%
2009	74%	75%	2020	81%	87%
2010	71%	77%			

5.2. Annual and Seasonal Variation of NDVI

As explained in previous sections, NDVI represents the greenness density and health of vegetation within each pixel of a satellite image. Figures 6 and 7 exemplify NDVI maps for five years (2000, 2005, 2010, 2015, and 2020) for the two seasons. The NDVI of the study area has changed considerably between 2000 and 2020 for both seasons. The wet season shows the highest NDVI values ranging between 0.34 and 0.74, with an average of 0.54, while, for the dry season, NDVI ranges between 0.42 and 0.64, with an average of 0.53 between 2000 to 2009. However, after dam construction, in the wet season, the highest NDVI values range between 0.39 and 0.69, with an average of 0.54, while, for the dry season, they range from 0.28 to 0.41, with an average of 0.34. This indicates a 26 percent decline in average NDVI for the dry season over the study area. Overall, the comparative analysis before and after dam construction shows higher NDVI values both in terms of magnitude and spatial distribution before the dam construction.

Preprints (www.preprints.org) | NOT PEER-REVIEWED | Posted: 8 August 2023 doi:10.20944/preprints202308.0566.v1

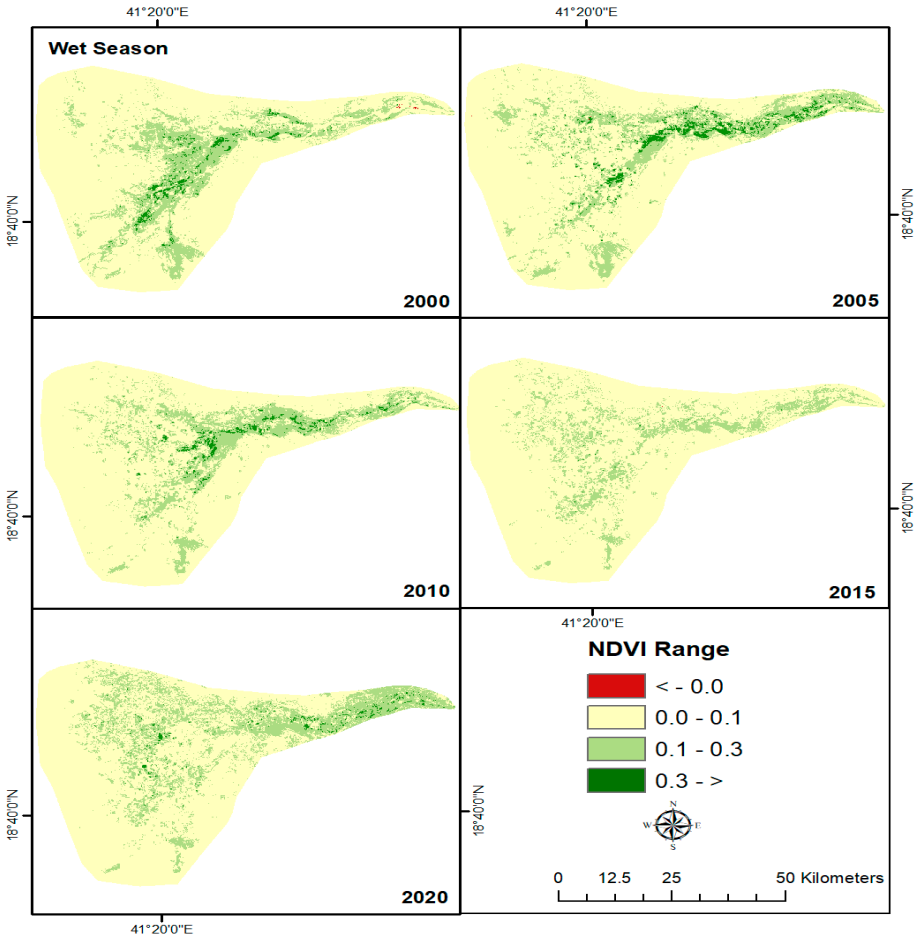

Figure 6. NDVI maps generated form Landsat 4,5,7, and 8 for wet seasons for 2000, 2005, 2010, 2015, and 2020.

NDVI variations are further analyzed to provide a clear understanding of how they vary over time. Spatially averaged NDVI time series from 2000 to 2020 for the wet and dry seasons were calculated from Landsat images and displayed in Figure 8a,b. The mean NDVI for wet and dry seasons before dam construction are 0.115 and 0.102, respectively. Moreover, the mean NDVI for wet and dry seasons after dam construction are 0.103 and 0.089, respectively. There was a variation in annual mean NDVI before dam construction. Before the dam construction, there was an increase of 0.0007 and 0.0019 in the NDVI values during the wet and dry seasons, respectively. Following dam construction, NDVI values experienced a decrease of 0.0027 and 0.0028 during wet and dry seasons, respectively. A clear decline in the mean NDVI values can be observed after the dam construction starting in 2010 and 2011 for both seasons. Before the dam construction, the trend in mean NDVI values slightly increased, which could be due to the amount of precipitation and a larger amount of surface runoff. A noticeable decrease, however, can be seen after the dam construction, especially during the dry season. This could be due to the restriction of water downstream of the dam, which may result in the reduction of regeneration and vegetation greenness, as can be seen in Figures 6 and 7.

Preprints (www.preprints.org) | NOT PEER-REVIEWED | Posted: 8 August 2023 doi:10.20944/preprints202308.0566.v1

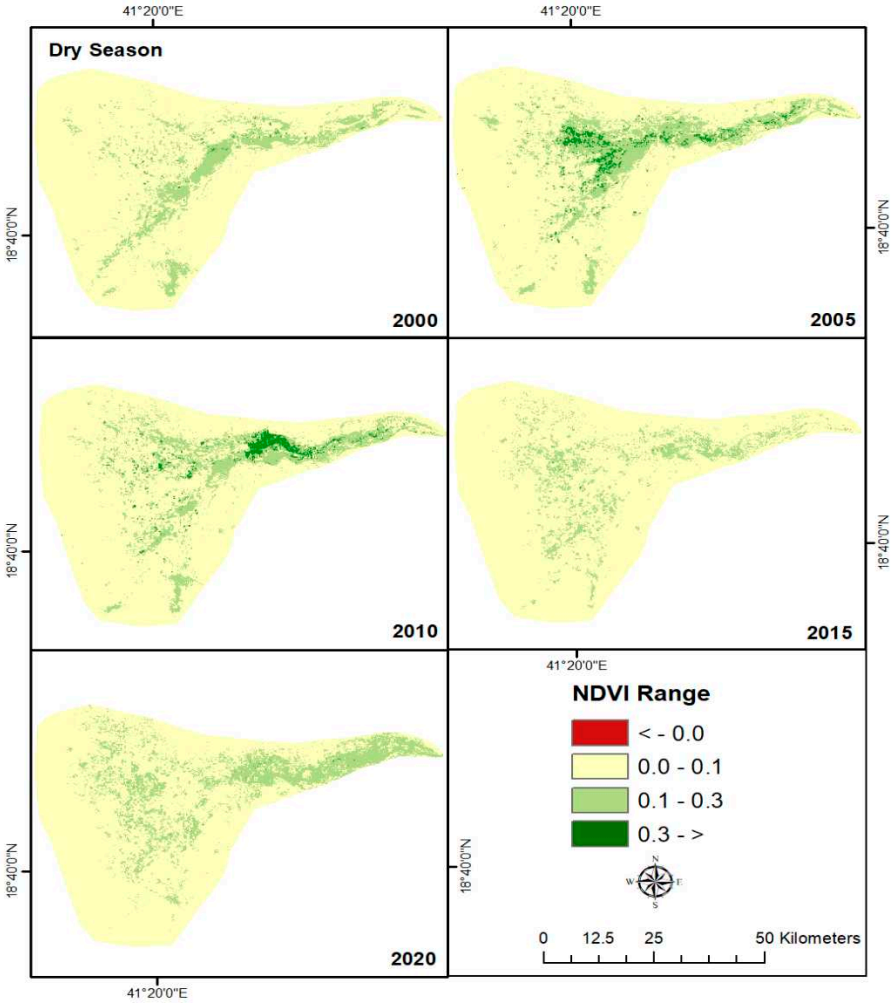

Figure 7. NDVI maps generated from Landsat 4,5,7, and 8 for dry seasons for 2000, 2005, 2010, 2015, and 2020.

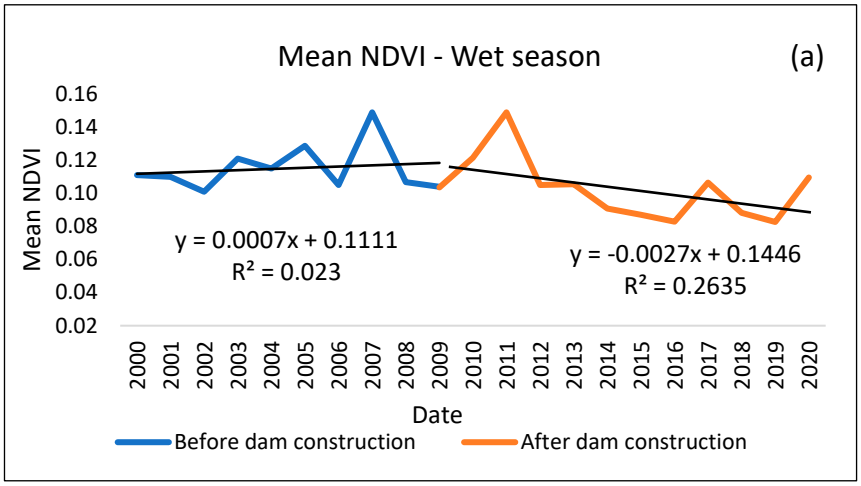

Preprints (www.preprints.org) | NOT PEER-REVIEWED | Posted: 8 August 2023 doi:10.20944/preprints202308.0566.v1

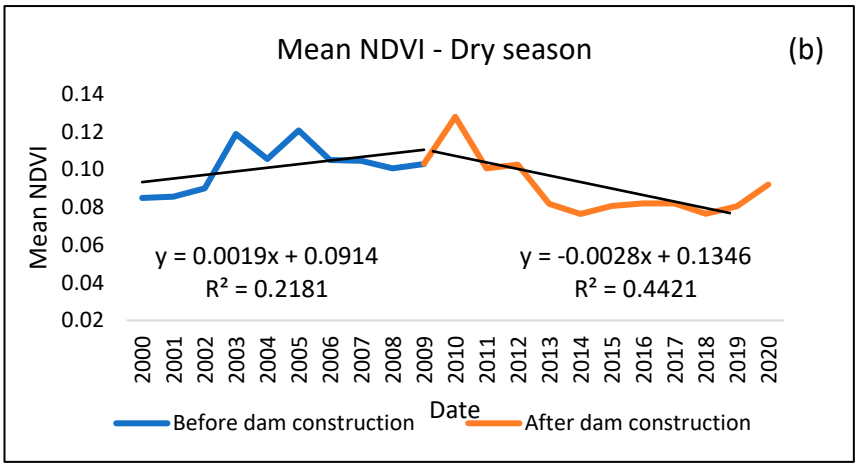

Figure 8. The mean NDVI trendlines for wet season (a) and dry season (b) variation from 2000 to 2020.

5.3. NDVI Changes

Figure 9 represents the gain and loss of downstream vegetation areas using the NDVI values. Based on the NDVI values for each season, Figure 9 shows the difference in the mean NDVI before and after the dam construction for the wet and dry seasons. The red color in Figure 9 represents the loss of vegetation areas downstream of the dam and mainly coincides with the natural vegetation. The green color in this figure represents the gain of vegetation areas downstream of the dam, which primarily corresponds to the croplands. The significant vegetation changes before and after dam construction for the two seasons are primarily in areas far from the dam, such as in the middle of the stream and the alluvial fan areas. The alluvial fan areas are deposits of gravel, sand, and even smaller sediment particles, such as silt (Dehwah et al., 2014). These areas are relatively fertile than other soil types. Therefore, the dam impounded this sediment to be transported by seasonal water flow from the Hail basin catchment to the downstream alluvial fan areas (Lopez et al., 2014), could impacting the vegetation areas downstream. The negative impact represented in red color, which mainly represents the natural vegetation area, could be due to several reasons; for example, may downstream wetland areas decrease due to the dam impoundment of water to support downstream vegetation areas. The gained areas mostly show the croplands, possibly due to the dam's irrigation water.

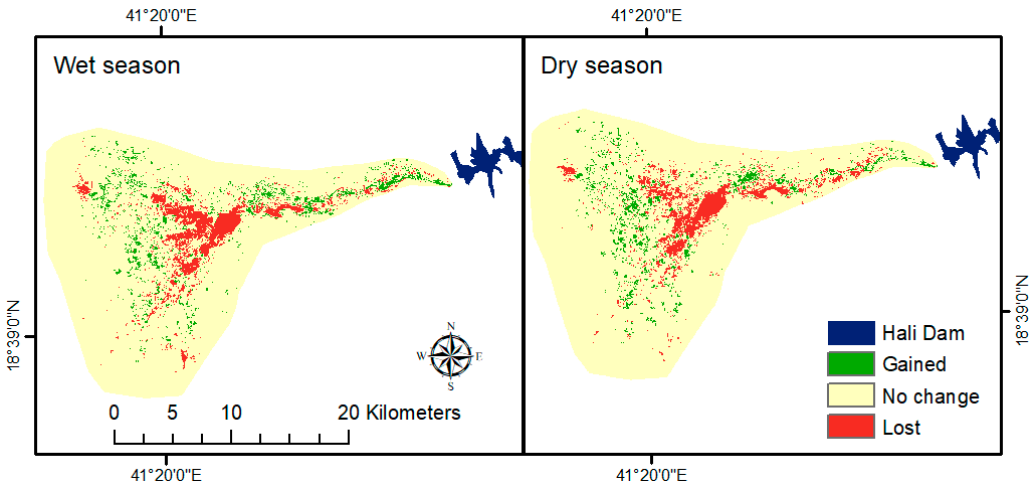

Figure 9. The spatial distribution of the differencing of NDVI before and after the dam construction for wet and dry seasons.

Preprints (www.preprints.org) | NOT PEER-REVIEWED | Posted: 8 August 2023 doi:10.20944/preprints202308.0566.v1

5.4. Inter-Annual Variations of Climatic Variables

5.4.1. Precipitation and temperature

To better investigate the vegetation trends and the potential impact of climate variabilities, we further used monthly climate model data from 2000 to 2020. The changes in the monthly two-meter surface temperature and total precipitation could be explain the observed changes in the mean NDVI. ERA-5 and GLDAS Climate data were obtained for the downstream areas of the case study. Figure 10a–c shows the total monthly two-meter surface temperature, precipitation, and mean NDVI of the study area from 2000 to 2020. Figure 10a shows the monthly two-meter surface temperature changes in the study area. No significant change in the average two-meter surface temperature before the dam construction (30.23°C) and after the dam construction (30.25°C) was found.

While some increase in the amount of total precipitation can be seen (e.g., in 2001 and 2004), the overall trend of precipitation is slightly negative from 2000 to 2015, which could, in turn, impact the mean NDVI (Figure 10c) and the vegetation areas variations. Moreover, EWT could contribute to the change in the variation of NDVI, as will be discussed in section 5.4.3. Almazroui et al. (2012) reported a similar decline for the Saudi Arabia's precipitation from 1994 to 2009. Moreover, Hasanean and Almazroui (2015) reported high precipitation accrued in 2001 and 2004 in the wet season. In 2016 and 2017, there was a high amount of precipitation in the study area. This could be due to the presence of temperature anomalies in this period (Almazroui, 2020) . The mean total monthly precipitation before and after the dam construction is relatively close: 3.05 mm and 2.88 mm, respectively. Despite slight changes in the precipitation and the two-meter surface temperature before and after the dam construction, these results show no clear evidence of climate variability on the area that could be responsible for the considerable observed vegetation decline after 2009.

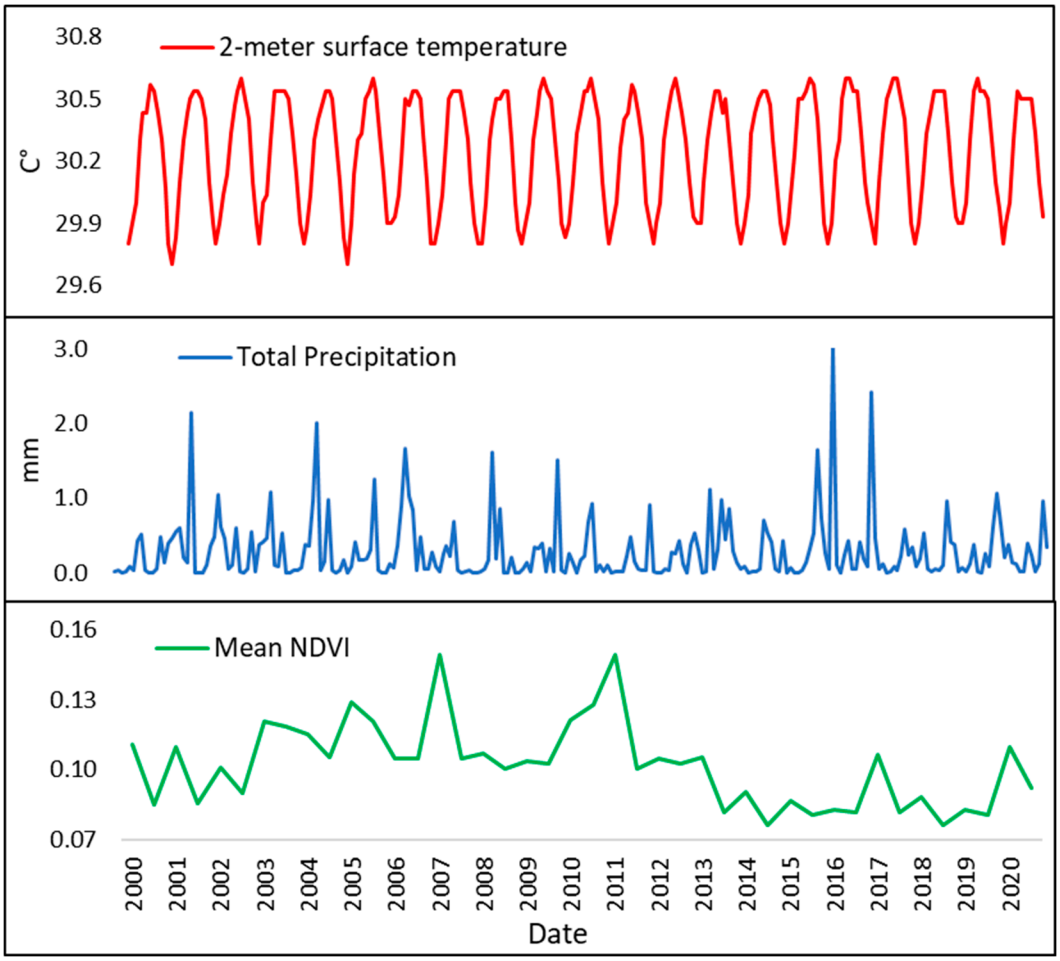

Figure 10. Two-meter surface temperature and total precipitation from 2000 to 2020 ERA-5 and mean NDVI.

Preprints (www.preprints.org) | NOT PEER-REVIEWED | Posted: 8 August 2023 doi:10.20944/preprints202308.0566.v1

5.4.2. Specific humidity and total evaporation

To further explore the impact of climate variability on the Wadi Hali downstream of the dam, total evaporation, and specific humidity are analyzed against the NDVI variations. Figure 11a shows the monthly total evaporation from 2000 to 2020, with negative values indicating evaporation and positive values indicating condensation. The total evaporation displays higher values in some years, such as 2016 and 2017. The increase in evaporation can be explained by higher precipitation values in 2016, and 2017. Overall, the variations in total evaporation are similar to the changes in total precipitation. Nevertheless, the mean total monthly evaporation before dam construction (−0.00031 m water equivalent) is slightly higher than after the construction of the dam (−0.00029 m water equivalent).

Figure 11b shows the monthly specific humidity, which refers to the quantity of water vapor contained in a unit quantity of air, expressed as kilograms of water vapor per kilogram of air. The average monthly specific humidity before the dam construction was 0.015 kg kg-1 and 0.016 kg kg-1 after the dam was constructed. Therefore, this increase is insignificant as it shows no overall considerable change in evaporation and specific humidity before and after the dam construction. This suggests that vegetation changes could be primarily related to the water (surface and subsurface) changes that could be impacted by the dam construction.

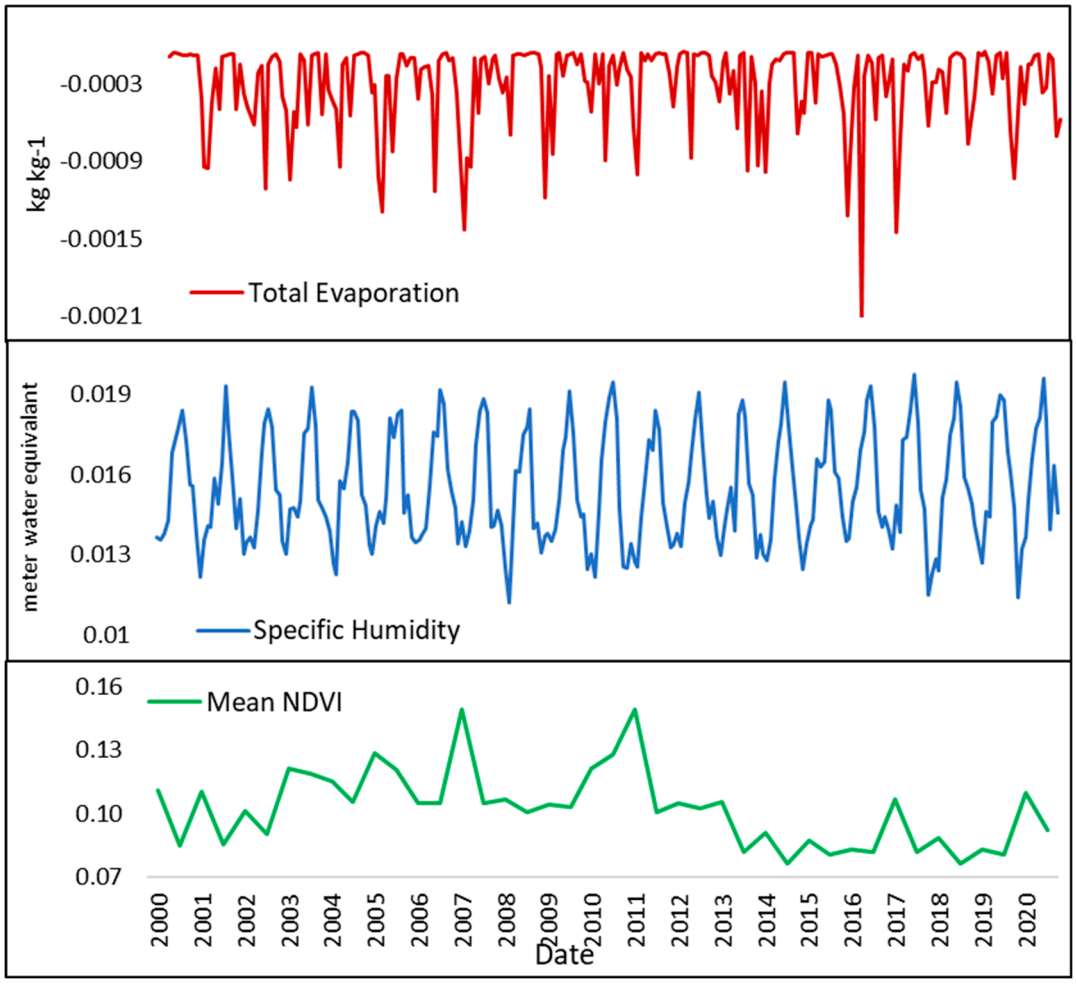

Figure 11. Total evaporation in meter water equivalent from 2000 to 2020 ERA-5 (a) and monthly specific humidity kg kg-1 from 2000 to 2020 GLDAS (b) with mean NDVI (c).

5.4.3. Annual variations of EWT

In order to investigate the effects of EWT and, specifically, soil moisture and groundwater changes in vegetation trends, we analyzed EWT data from 2002 to 2020. Figure 12 represents the monthly EWT in the land, with a clear negative trend from 2005 to 2020. Except for some seasonal

Preprints (www.preprints.org) | NOT PEER-REVIEWED | Posted: 8 August 2023 doi:10.20944/preprints202308.0566.v1

variations and strong anomalies (e.g., in 2017), the EWT overall changes and trends, particularly after 2009, are different than climate variables changes, such as precipitation and evaporation. EWT and mean NDVI increased between 2002 and 2007, while precipitation decreased. A similar relationship was observed in several other studies, such as during periods of no precipitation, soil-water content increases and was attributed to a variety of environmental and climatic factors (Guillod et al., 2015; Sehler et al., 2019). A clear reduction in both EWT and the mean NDVI exists after 2003 and 2011 respectively. The reduction in the EWT could be due to agriculture's continuous depletion of groundwater over the past years (Alrwis et al., 2021). It is expected that the EWT and NDVI time series share similar variations since there is a close relationship between soil moisture variations and vegetation changes. Overall, changes in EWT were negatively impacted by decreasing rainfall, dam construction, and high depletion by anthropogenic activities of groundwater, which consequently affected vegetation changes and water stored in the land.

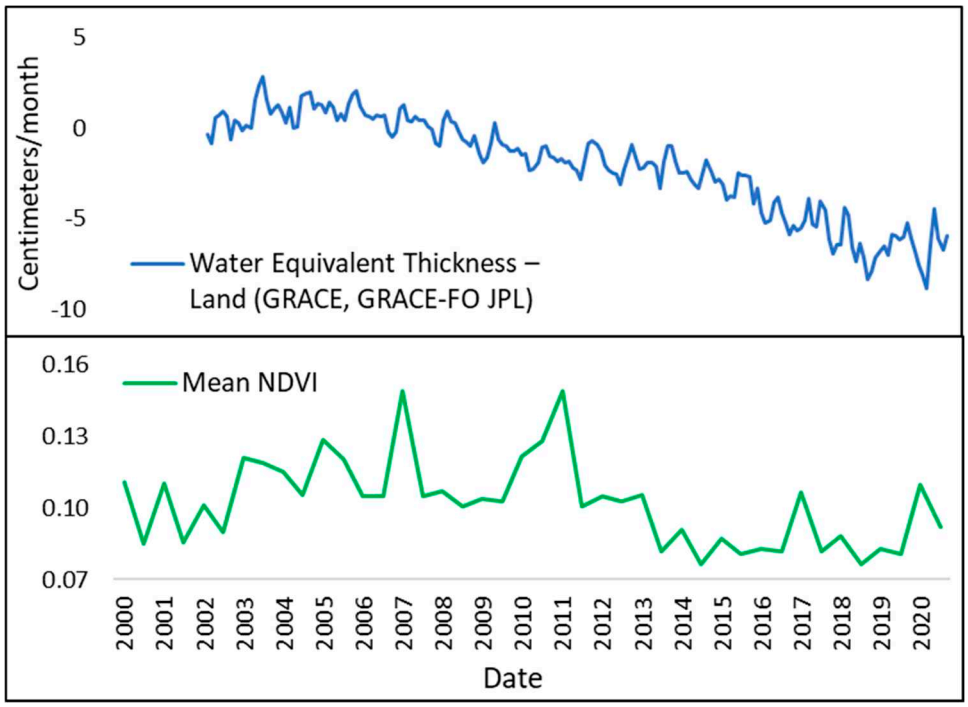

Figure 12. Equivalent Water Thickness (EWT) centimeters/month from 2002 to 2020 GRACE with mean NDVI.

5.5. Correlation Coefficient Analysis

Climate variables and soil water availability are the main driving forces for vegetation (Yang et al., 2019). In this section, the Pearson correlation values between NDVI, natural vegetation, croplands, climatic variables (i.e. precipitation, evaporation, temperature, and humidity), and EWT are presented. Table 2 shows the results of the applied Pearson Correlation Coefficient to test the Pearson correlation between different variables and mean NDVI, cropland and natural vegetation areas, before and after dam construction for wet and dry seasons. Table 2 shows a strong positive correlation ranging from 0.66 to 0.80, with a significant $p<0.05$ between vegetation types and NDVI with precipitation for the wet season before dam construction. Moreover, a moderate to strong positive correlation ($p<0.05$ for only natural vegetation) between vegetation types and NDVI with two-meter surface temperature in the dry season before dam construction.

Evaporation correlation with vegetation areas and NDVI, as shown in Table 2, mainly follows the precipitation correlation values. For example, in the wet season, as the precipitation correlation became strongly positive, the evaporation became strongly negative with vegetation areas and NDVI. Regarding the specific humidity, the correlation between vegetation areas and humidity is ambiguous due to climate characteristics in an arid area. After dam construction for both seasons, the

Preprints (www.preprints.org) | NOT PEER-REVIEWED | Posted: 8 August 2023 doi:10.20944/preprints202308.0566.v1

Pearson correlation between vegetation changes and climate variables is mostly very low. Nevertheless, strong correlations can be seen between EWT and both vegetation types and NDVI after the dam construction. These Pearson correlation values agree with the previously presented results where NDVI variations follow climate variables patterns before 2009. However, lower Pearson correlations can be seen after the dam construction, especially during the dry seasons. The pattern of NDVI variations is different and better match those of EWT (cf. Figures 10–12). This can be explained by the impact of the dam on the downstream soil moisture and groundwater changes, as well as groundwater withdrawal for agriculture which are better reflected in the EWT data. The difference in the Pearson correlations before and after dam construction could also be due to the impoundment of water flow by the dam construction.

Table 2. Pearson correlation and p-value of vegetation type and NDVI with climate variables and EWT.

	Precipitation		Evaporation		Temperature		Humidity		EWT	
Before Dam Construction: Wet season										
	R	P	R	P	R	P	R	P	R	P
Natural vegetation	**0.77**	0.009	**-0.77**	0.009	-0.36	0.312	-0.05	0.989	0.10	0.820
croplands	**0.66**	0.039	**-0.58**	0.082	-0.33	0.353	-0.08	0.822	-0.30	0.467
Mean NDVI	**0.80**	0.005	**-0.76**	0.011	-0.14	0.708	0.42	0.232	0.24	0.566
After Dam Construction: Wet season										
	Precipitation		Evaporation		Temperature		Humidity		EWT	
	R	P	R	P	R	P	R	P	R	P
Natural vegetation	0.04	0.899	0.41	0.207	0.03	0.941	**-0.52**	0.103	**0.57**	0.065
croplands	0.04	0.916	0.29	0.382	0.22	0.516	**0.62**	0.040	**-0.66**	0.023
Mean NDVI	0.03	0.927	0.20	0.557	-0.13	0.697	-0.17	0.612	**0.50**	0.157
Before Dam Construction: Dry season										
	Precipitation		Evaporation		Temperature		Humidity		EWT	
	R	P	R	P	R	P	R	P	R	P
Natural vegetation	0.28	0.430	0.45	0.188	**0.72**	0.019	0.25	0.477	0.34	0.125
croplands	-0.25	0.487	0.23	0.524	**0.54**	0.330	-0.56	0.092	-0.50	0.204
Mean NDVI	-0.07	0.851	-0.10	0.775	**0.56**	0.090	0.13	0.704	0.11	0.790
After Dam Construction: Dry season										
	Precipitation		Evaporation		Temperature		Humidity		EWT	
	R	P	R	P	R	P	R	P	R	P
Natural vegetation	0.12	0.715	-0.10	0.762	-0.28	0.400	0.29	0.376	0.48	0.276
croplands	0.11	0.740	-0.05	0.893	0.42	0.199	0.38	0.245	-0.49	0.155
Mean NDVI	-0.17	0.626	0.27	0.428	-0.18	0.595	-0.28	0.395	0.50	0.143

5.6. Multivariate Regression Analysis

The variations in the climate variables and the amount of soil water are largely reflected in the total vegetation area. To investigate this more deeply in the case study, multivariant linear regression is used to assess the variations of EWT and climate variables on NDVI variations before (2000–2009) and after (2010–2020) the dam construction. This is done in two different scenarios: (1) modeling NDVI only based on climate variables (i.e., precipitation, two-meter surface temperature, evaporation, and specific humidity without EWT) and (2) modeling NDVI using all variables including EWT. This is done to examine the impact of EWT on NDVI changes that were found to be considerable in previous sections. In the multivariant linear regression model, NDVI is considered a

Preprints (www.preprints.org) | NOT PEER-REVIEWED | Posted: 8 August 2023 doi:10.20944/preprints202308.0566.v1

dependent variable, while EWT and climate variables are independent variables that drive the variation of NDVI.

Figures 15A,B show the results of multivariant linear regression applied to assess the variations of the NDVI using only climate variables before (Figures 15A) and after (Figures 15B) the dam construction. The R^2 value is found to be 0.76 before the dam construction from 2002 to 2009 between the observed and modelled NDVI. It indicates 76 percent of the variations in NDVI before the dam construction was driven by climate variables. On the other hand, the Pearson correlation between observed and modeled NDVI after the dam construction is very weak. The R^2 value is 0.22 after the dam construction from 2010 to 2020. Therefore, using only climate variables to model the variation of NDVI is mainly useful before the dam construction but not after. EWT data may be essential for modelling the variation of the NDVI that suggests the important role of groundwater and soil moisture.

Figure 13 demonstrates the results of the second scenario, where all variables, including EWT, are used to predict the NDVI variations. As in Figure 13A, the Pearson correlation between observed and predicted mean NDVI before the dam construction is strong in the case study. The R^2 value is 0.85 before the dam construction from 2002 to 2009. It indicates 85 percent of the variations in NDVI before the dam construction was driven by climate variables and EWT. This, which is higher than the first scenario where only climate variables were assumed, clearly shows an impact of the water stored in the land on the vegetations. After the dam construction, the correlation between observed and modeled NDVI after the dam construction is weak (Figure 13B). Nevertheless, the R^2 value (0.42) is higher than the first scenario after the dam construction from 2010 to 2020. It indicates that while adding EWT to the variables increases the correlation between the modelled and observed NDVI, a considerable discrepancy between the NDVI variations and other variables exists. Overall, NDVI variations do not follow the climatic pattern as they did before dam construction. The changes in the correlation before and after the dam construction could be due to changes in the downstream ecosystem. The dam construction impoundment of the seasonal water flow may contribute to a decrease in the R^2 to 0.42.

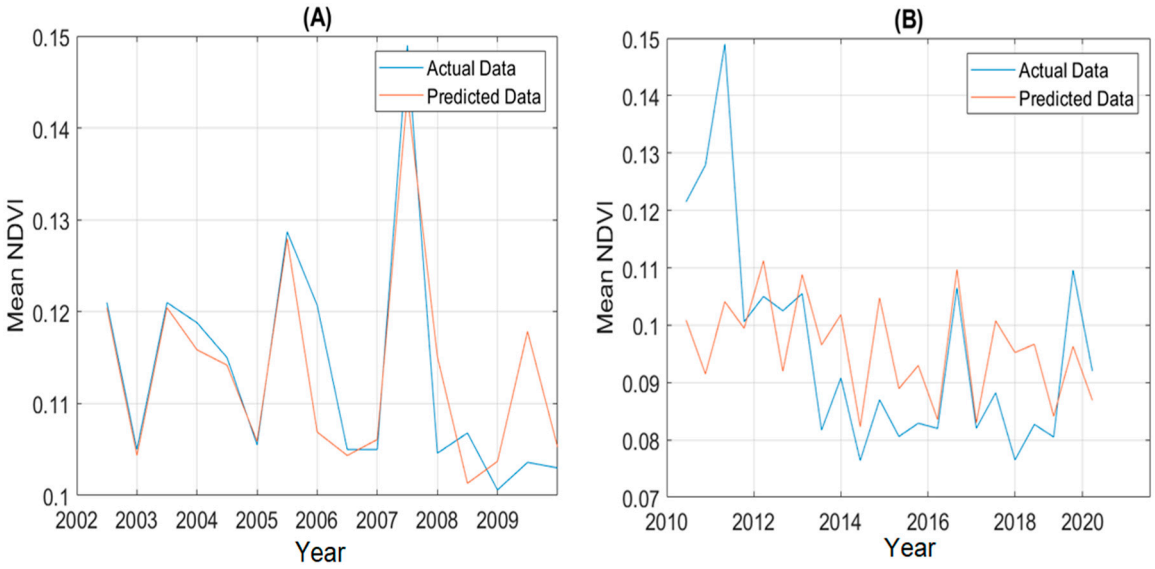

Figure 13. Modelling the mean NDVI variations using only climate variables data including 2-meter surface temperature, total precipitation, total evaporation, and specific humidity before the dam construction 2002 to 2009 as number (A) and after the dam construction 2010 to 2020 as number (B).

6. Discussion

Based on Figures 3–5, croplands have been increasing since 2009 as one of the important purposes of the dam. Results suggest that human activities and croplands influenced by the dam have been extended at the expense of natural vegetation. Such activities, however, should be studied

 doi:10.20944/preprints202308.0566.v1

in more details in studies. The NDVI time series and trends, as shown in Figures 6–8, have a decreasing trend for both wet and dry seasons after dam construction. Moreover, the inter-annual vegetation NDVI and natural vegetation have declined significantly after the dam construction. A considerable difference was found in the correlation between natural vegetation, croplands, and mean NDVI with climate variables before and after dam construction, which could be explained by the impact of the dam on the region's environment. Prior to dam construction, NDVI and vegetation types in the study area were highly correlated with surface temperatures and total precipitation for both seasons. These results agree with the relevant literature. For example, Xie et al. (2016) and Tong et al. (2018) suggest a strong positive correlation between vegetation and climate variables, especially for precipitation and temperature, which is similar to our findings before dam construction. However, after the dam construction, the correlation between vegetation and climate variables was much lower, especially for the total precipitation, which are critical climate variables for vegetation area. Such correlation decrease can be due to the dam's impacts. For example, stopping seasonal water flow to the study area could influence vegetation growth and distribution in the study area. Before dam construction, precipitation and particularly seasonal runoff water from the eastern mountains were the primary sources of vegetation area and soil moisture. Disrupting the runoff via the application of the Hali Dam was found to significantly affect vegetation growth and greenness. Moreover, high temperatures and rapid evaporation can limit the water absorption from the precipitation by the soil in the areas.

The slight changes in the climate variables, as shown in Figures 11–13, may lead to slight changes in the vegetation area. However, more significant changes in human activities, e.g., through the dam construction can cause similar changes in the total vegetation area. Despite slight changes in the precipitation and two-meter surface temperature before and after dam construction, these results show no clear evidence of the climate variability impacts on the area and, correspondingly, the vegetation decline after 2009. Regarding the cropland expansion and decrease in the EWT, there are several papers that have examined the relationship between groundwater use and cropland expansion in Saudi Arabia. A comprehensive study was conducted by the International Water Management Institute (IWMI) (IWMI, 2014). The study found that groundwater use has been a major driver of cropland expansion in Saudi Arabia since the 1970s. The study also found that the expansion of cropland has led to a decline in the groundwater in many parts of the country. Another study by Alshehri and Mohamed (2023) indicates that the agriculture sector was largely responsible for the dramatic increase in groundwater extraction in Tabuk areas, which clearly shows a decline in the EWT.

This study was able to identify a noticeable link between the NDVI and both climate variables and EWT variations. According to Figure 13A, using only climate variables one could model the NDVI variation to a high degree before the dam construction. This modeling can be performed more successfully with a combination of climate variables and EWT before the dam construction (cf. Figure 14A). However, Figures 13B suggests that climate variables only were not able to accurately model the variation of the mean NDVI after dam construction. Adding the EWT data, however, can improve the modeling skill to some extent (Figure 14B). Including EWT as the influencing factor in the multivariate regression analysis led to improved results with a higher R^2 value, which is important in estimating and representing the role of groundwater and soil moisture (Tangdamrongsub et al., 2018). According to the literature, EWT can be used to represent the impact of human variables on the total vegetation area (Liu et al., 2021; Pan et al., 2017). In Pan et al. (2017), human-induced evapotranspiration was detected in the Haihe River basin of China using EWT. Based on their findings, GRACE has the capability to detect anthropogenic signals over regions with high groundwater consumption. The use of underground water for irrigation, water flow prevention by dam construction, and decreased soil moisture can lead to a negative trend in the EWT time series. Correspondingly, this can impact the total vegetation area directly by limiting soil moisture and increasing sand movement and soil salinity. EWT contributes to the increased vegetation greenness independent of climate variables.

Preprints (www.preprints.org) | NOT PEER-REVIEWED | Posted: 8 August 2023 doi:10.20944/preprints202308.0566.v1

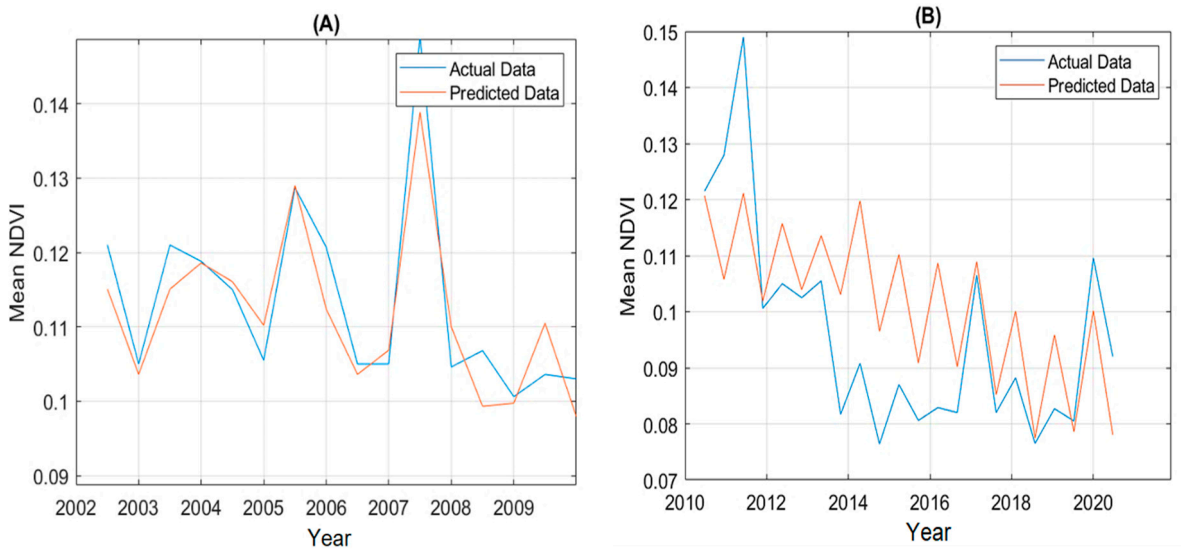

Figure 14. Modelling the mean NDVI variations using EWT and climate variables data including 2-meter surface temperature, total precipitation, total evaporation, and specific humidity before the dam construction 2002 to 2009 as number (A) and after the dam construction 2010 to 2020 as number (B).

7. Conclusion

The function of dams and related reservoirs in arid areas is indispensable both to human society and nature. Their primary purpose is to alter the characteristics of the land surface and increase the proportion of the water surface, especially in arid regions. Based on the characteristics of the selected study area, dam, and related reservoirs, and using 21-year (i.e., 2000–2020) meteorological and remote sensing data, this study aimed to detect changes in vegetation areas downstream of Hali Dam in the Wadi Hali basin. NDVI results reveal a considerable decline after the dam construction in the dry season. This is primarily associated with blocking the seasonal runoff water by the dam and increasing cropland areas due to dam irrigation. There was no significant change in climate variables before and after the dam construction, which shows no clear evidence of the climate variability impacts on the area and, correspondingly, the vegetation decline after 2009. A significantly stronger correlation between vegetation changes and precipitation and temperature variations is observed before dam construction. According to the multivariate regression analysis, 85 percent of the variations in the mean NDVI were driven by climate variables and EWT. On the other hand, it was found that only 42 percent of the variations in NDVI were driven by climate variables and EWT from 2010 to 2020 for both dry and wet seasons. Another analysis by the multivariate regression analysis using only the climate variables to model the NDVI variations shows that, before dam construction, climate variables may have caused the variation of the NDVI values (with an R^2 of 0.76) but not after dam construction (with an R^2 of 0.22). Other factors that impact downstream vegetation areas, such as Land Use Land Cover (LULC), soil components, wetlands, and groundwater, are important to be considered in future research. Using high spatial resolution satellite imagery or combining high spatial resolution with medium spatial resolution is essential for a small study area and can improve accuracy assessment values. To address this study's limitation and future work, it is essential to consider other factors that impact downstream vegetation area, such as Land Use Land Cover (LULC), soil components, wetlands, and groundwater. Climate variables do not have a significant impact, whereas other variables could have more impact on downstream vegetation area.

Author Contributions: Conceptualization, R.A. and M.K.; methodology, R.A.; writing—original draft preparation, R.A.; writing—review and editing, M.K., P.M.S. and J.F.R.; visualization, R.A.; supervision, M.K., P.M.S. and J.F.R.; project administration, R.A. All authors have read and agreed to the published version of the manuscript.

Contribution Statement: Raid Almalki: Conceptualization, Investigation, Methodology, Data curation, Formal analysis, Visualization, Writing – original draft. Mehdi Khaki: Supervision, Conceptualization, Investigation, Writing – review & editing. Patricia M. Saco: Supervision, Conceptualization, Writing – review & editing. Jose F. Rodriguez: Supervision, Conceptualization, Writing – review & editing.

Funding: This study received no external funding.
Data Availability Statement: Not applicable.

Acknowledgments: R.A. would like to express my sincere gratitude to Umm Al-Qura University for its funding and encouragement.

Conflicts of Interest: The authors declare no conflict of interest.

References

Ahmed, S. (2018). Assessment of urban heat islands and impact of climate change on socioeconomic over Suez Governorate using remote sensing and GIS techniques. *The Egyptian Journal of Remote Sensing and Space Science*, *21*(1), 15-25.

Alarifi, S. S., Abdelkareem, M., Abdalla, F., & Alotaibi, M. (2022). Flash Flood Hazard Mapping Using Remote Sensing and GIS Techniques in Southwestern Saudi Arabia. *Sustainability*, *14*(21), 14145.

Almalki, R., Khaki, M., Saco, P. M., & Rodriguez, J. F. (2022). Monitoring and Mapping Vegetation Cover Changes in Arid and Semi-Arid Areas Using Remote Sensing Technology: A Review. *Remote Sensing*, *14*(20), 5143.

Almazroui, M. (2020). Changes in temperature trends and extremes over Saudi Arabia for the period 1978–2019. *Advances in Meteorology*, *2020*.

Alrwis, K. N., Ghanem, A. M., Alnashwan, O. S., Al Duwais, A. A. M., Alaagib, S. A. B., & Aldawdahi, N. M. (2021). Measuring the impact of water scarcity on agricultural economic development in Saudi Arabia. *Saudi Journal of Biological Sciences*, *28*(1), 191-195.

Alshehri, F., & Mohamed, A. (2023). Analysis of Groundwater Storage Fluctuations Using GRACE and Remote Sensing Data in Wadi As-Sirhan, Northern Saudi Arabia. *Water*, *15*(2), 282.

Belal, A.-A., El-Ramady, H. R., Mohamed, E. S., & Saleh, A. M. (2014). Drought risk assessment using remote sensing and GIS techniques. *Arabian Journal of Geosciences*, *7*(1), 35-53.

Bhandari, A., Kumar, A., & Singh, G. (2012). Feature extraction using Normalized Difference Vegetation Index (NDVI): A case study of Jabalpur city. *Procedia technology*, *6*, 612-621.

Borsa, A. A., Agnew, D. C., & Cayan, D. R. (2014). Ongoing drought-induced uplift in the western United States. *Science*, *345*(6204), 1587-1590.

Chen, P. (2015). *Material Science and Environmental Engineering: Proceedings of the 3rd Annual 2015 International Conference on Material Science and Environmental Engineering (ICMSEE2015, Wuhan, Hubei, China, 5-6 June 2015)*. CRC Press.

Congalton, R. G. (1991). A review of assessing the accuracy of classifications of remotely sensed data. *Remote Sensing of Environment*, *37*(1), 35-46.

Degu, A. M., Hossain, F., Niyogi, D., Pielke Sr, R., Shepherd, J. M., Voisin, N., & Chronis, T. (2011). The influence of large dams on surrounding climate and precipitation patterns. *Geophysical Research Letters*, *38*(4).

Dehwah, A. H., Al-Mashharawi, S., & Missimer, T. M. (2014). Mapping to assess feasibility of using subsurface intakes for SWRO, Red Sea coast of Saudi Arabia. *Desalination and Water Treatment*, *52*(13-15), 2351-2361.

Foody, G. (2003). Geographical weighting as a further refinement to regression modelling: An example focused on the NDVI–rainfall relationship. *Remote Sensing of Environment*, *88*(3), 283-293.

Gandhi, G. M., Parthiban, b., Thummalu, N., & Christy, A. (2015). Ndvi: Vegetation change detection using remote sensing and gis–A case study of Vellore District. *Procedia computer science*, *57*, 1199-1210.

Guarino, L., & Al-Juwaeid, A. A. (1990). Wheat collecting in Saudi Arabia. *2 FOOD AND AGRICULTURE ORGANIZATION OF THE UNITED NATIONS@ ORGANISATION DES NATIONS UNIES POUR L'ALIMENTATION ET L'AGRICULTURE ORGANIZACION DE LAS NACIONES UNIDAS PARA LA AGRICULTURA Y LA ALIMENTACION*, 36.

Guillod, B. P., Orlowsky, B., Miralles, D. G., Teuling, A. J., & Seneviratne, S. I. (2015). Reconciling spatial and temporal soil moisture effects on afternoon rainfall. *Nature Communications*, *6*(1), 6443.

Han, F., Yan, J., & Ling, H.-b. (2021). Variance of vegetation coverage and its sensitivity to climatic factors in the Irtysh River basin. *PeerJ*, *9*, e11334.

Hasanean, H., & Almazroui, M. (2015). Rainfall: features and variations over Saudi Arabia, a review. *Climate*, *3*(3), 578-626.

Hu, M. Q., Mao, F., Sun, H., & Hou, Y. Y. (2011). Study of normalized difference vegetation index variation and its correlation with climate factors in the three-river-source region. *International Journal of Applied Earth Observation and Geoinformation*, *13*(1), 24-33.

IWMI. (2014). Strategy 2014–2018—Solutions for a water-secure world. In: International Water Management Institute Colombo.

Ji, L., & Peters, A. J. (2004). A spatial regression procedure for evaluating the relationship between AVHRR-NDVI and climate in the northern Great Plains. *International journal of remote sensing*, *25*(2), 297-311.

Jiang, M., Tian, S., Zheng, Z., Zhan, Q., & He, Y. (2017). Human activity influences on vegetation cover changes in Beijing, China, from 2000 to 2015. *Remote Sensing*, *9*(3), 271.

Khaki M., Forootan, E., Sharifi, M.A., Awange, J., Kuhn, M. (2015). Improved gravity anomaly fields from retracked multimission satellite radar altimetry observations over the Persian Gulf and the Caspian Sea, Geophysical Journal International, Volume 202, Issue 3, Pages 1522–1534, https://doi.org/10.1093/gji/ggv240

Khaki M., Hoteit, I. (2021). Monitoring water storage decline over the Middle East, Journal of Hydrology, Volume 603, Part D, 127166, ISSN 0022-1694, https://doi.org/10.1016/j.jhydrol.2021.127166.

Kumari,N., Saco,P.M., Rodriguez,J.F., Johnstone,S.A.,Srivastava,A.,& Chun,K.P.,et al. (2020).The grass is not always greener on the other side: Seasonal reversal of vegetation greeness in aspect-driven semiarid ecosystems.Geophysical Research Letters,47,e2020GL088918.https://doi. org/10.1029/2020GL088918

Li, L., Ustin, S. L., & Lay, M. (2005). Application of AVIRIS data in detection of oil-induced vegetation stress and cover change at Jornada, New Mexico. *Remote Sensing of Environment*, *94*(1), 1-16.

Liu, B., Zou, X., Yi, S., Sneeuw, N., Cai, J., & Li, J. (2021). Identifying and separating climate-and human-driven water storage anomalies using GRACE satellite data. *Remote Sensing of Environment*, *263*, 112559.

Lopez, O., Stenchikov, G., & Missimer, T. (2014). Water management during climate change using aquifer storage and recovery of stormwater in a dunefield in western Saudi Arabia. *Environmental Research Letters*, *9*(7), 075008.

Miller, N. L., Jin, J., & Tsang, C. F. (2005). Local climate sensitivity of the Three Gorges Dam. *Geophysical Research Letters*, *32*(16).

Mohajane, M., Essahlaoui, A., Oudija, F., Hafyani, M. E., Hmaidi, A. E., Ouali, A. E., Randazzo, G., & Teodoro, A. C. (2018). Land use/land cover (LULC) using landsat data series (MSS, TM, ETM+ and OLI) in Azrou Forest, in the Central Middle Atlas of Morocco. *Environments*, *5*(12), 131.

Morgounov, A., Abubakr, M., Alhendi, A., Alkhatran, A., Alhuwaymil, H., & Ghosh, K. (2022). Agroclimatic Zones and Cropping Systems in the Southwestern Regions of the Kingdom of Saudi Arabia: Characterization, Classification and Improvement Potential. *Crops*, *2*(2), 186-201.

Murray H, Khaki M. (2021). Analysis of Surface Water Areal changes using Remote Sensing Data. Adv Environ Eng Res; 2(3): 019; doi:10.21926/aeer.2103019.

Nageswara Rao, P., Shobha, S., Ramesh, K., & Somashekhar, R. (2005). Satellite-based assessment of agricultural drought in Karnataka state. *Journal of the Indian society of remote sensing*, *33*(3), 429-434.

Otukei, J. R., & Blaschke, T. (2010). Land cover change assessment using decision trees, support vector machines and maximum likelihood classification algorithms. *International Journal of Applied Earth Observation and Geoinformation*, *12*, S27-S31.

Pan, Y., Zhang, C., Gong, H., Yeh, P. J. F., Shen, Y., Guo, Y., Huang, Z., & Li, X. (2017). Detection of human-induced evapotranspiration using GRACE satellite observations in the Haihe River basin of China. *Geophysical Research Letters*, *44*(1), 190-199.

Richards, J. A., & Richards, J. (1999). *Remote sensing digital image analysis* (Vol. 3). Springer.

Sehler, R., Li, J., Reager, J., & Ye, H. (2019). Investigating relationship between soil moisture and precipitation globally using remote sensing observations. *Journal of Contemporary Water Research & Education*, *168*(1), 106-118.

Shi, Y., Shen, Y., Kang, E., Li, D., Ding, Y., Zhang, G., & Hu, R. (2007). Recent and future climate change in northwest China. *Climatic change*, *80*(3), 379-393.

Soepboer, W., Sugita, S., & Lotter, A. F. (2010). Regional vegetation-cover changes on the Swiss Plateau during the past two millennia: A pollen-based reconstruction using the REVEALS model. *Quaternary Science Reviews*, *29*(3-4), 472-483.

Srivastava, S., Jayaraman, V., Nageswara Rao, P., Manikiam, B., & Chandrasekhar, M. (1997). Interlinkages of NOAA/AVHRR derived integrated NDVI to seasonal precipitation and transpiration in dryland tropics. *International journal of remote sensing*, *18*(14), 2931-2952.

Tangdamrongsub, N., Han, S.-C., Decker, M., Yeo, I.-Y., & Kim, H. (2018). On the use of the GRACE normal equation of inter-satellite tracking data for estimation of soil moisture and groundwater in Australia. *Hydrology and Earth System Sciences*, *22*(3), 1811-1829.

Tong, S., Zhang, J., Bao, Y., Lai, Q., Lian, X., Li, N., & Bao, Y. (2018). Analyzing vegetation dynamic trend on the Mongolian Plateau based on the Hurst exponent and influencing factors from 1982–2013. *Journal of Geographical Sciences*, *28*(5), 595-610.

Tranmer, M., & Elliot, M. (2008). Multiple linear regression. *The Cathie Marsh Centre for Census and Survey Research (CCSR)*, *5*(5), 1-5.

Wang, J., Rich, P. M., & Price, K. P. (2003). Temporal responses of NDVI to precipitation and temperature in the central Great Plains, USA. *International journal of remote sensing*, *24*(11), 2345-2364.

Wu, L., Zhang, Q., & Jiang, Z. (2006). Three Gorges Dam affects regional precipitation. *Geophysical Research Letters*, *33*(13).

Xie, B., Jia, X., Qin, Z., Shen, J., & Chang, Q. (2016). Vegetation dynamics and climate change on the Loess Plateau, China: 1982–2011. *Regional Environmental Change*, *16*(6), 1583-1594.

Xie, Z., Huete, A., Cleverly, J., Phinn, S., McDonald-Madden, E., Cao, Y., & Qin, F. (2019). Multi-climate mode interactions drive hydrological and vegetation responses to hydroclimatic extremes in Australia. *Remote Sensing of Environment*, *231*, 111270.

Xu, Y., Yang, J., & Chen, Y. (2016). NDVI-based vegetation responses to climate change in an arid area of China. *Theoretical and Applied Climatology*, *126*(1), 213-222.

Yang, X.-D., Ali, A., Xu, Y.-L., Jiang, L.-M., & Lv, G.-H. (2019). Soil moisture and salinity as main drivers of soil respiration across natural xeromorphic vegetation and agricultural lands in an arid desert region. *Catena*, *177*, 126-133.

Zaidi, S. M., Akbari, A., Abu Samah, A., Kong, N. S., Gisen, A., & Isabella, J. (2017). Landsat-5 Time Series Analysis for Land Use/Land Cover Change Detection Using NDVI and Semi-Supervised Classification Techniques. *Polish Journal of Environmental Studies*, *26*(6).

Zhao, Y., Liu, S., & Shi, H. (2021). Impacts of dams and reservoirs on local climate change: a global perspective. *Environmental Research Letters*, *16*(10), 104043.

Zhong, L., Ma, Y., Hu, Z., Fu, Y., Hu, Y., Wang, X., Cheng, M., & Ge, N. (2019). Estimation of hourly land surface heat fluxes over the Tibetan Plateau by the combined use of geostationary and polar-orbiting satellites. *Atmospheric Chemistry and Physics*, *19*(8), 5529-5541.

Zhou, W., Gang, C., Zhou, L., Chen, Y., Li, J., Ju, W., & Odeh, I. (2014). Dynamic of grassland vegetation degradation and its quantitative assessment in the northwest China. *Acta Oecologica*, *55*, 86-96.